SUPPLEMENTARY MATERIALS

Aberrant Lipid Metabolism Disrupts Calcium Homeostasis Causing Liver ER Stress in Obesity

Suneng Fu, Ling Yang, Ping Li, Oliver Hofmann, Lee Dicker, Winston Hide, Xihong Lin, Steven M. Watkins, Alexander Ivanov, and Gökhan S. Hotamisligil

List of Supplementary Materials:

11, Supplementary Table 1: The liver ER proteome of lean and obese (ob/ob) mouse;

12, Supplementary Table 2a and 2b: The differentially regulated proteins in the lean and obese ER proteome;

13, Supplementary Table 3: The lipid compositions of diet consumed by mice and ER samples of lean and obese (ob/ob) mouse livers;

14, Supplementary Table 4: The ER lipid composition of obese mouse liver following the administration of *Pemt* or *lacZ* shRNA control viruses;

15, Supplementary Table 5: Fatty acid composition differences in the ER of obese liver following the administration of *Pemt* or *lacZ* shRNA Control viruses;

16, Supplementary Table 6: Oligonucleotide sequences used in this study.

FULL METHODS

Animals

Male leptin deficient (*ob/ob*) and wild type littermates in the C57BL/6J background were bred in house and used for all biochemical experiments. Leptin deficient mice used for adenovirus-mediated expression experiments were purchased from the Jackson Laboratory (strain B6.V-Lep^{ob}/J, stock number 000632). All mice were maintained on a 12-hour-light /12-hour-dark cycle in a pathogen-free barrier facility with free access to water and regular chow diet containing 2200ppm of choline (PicoLab® Mouse Diet 20).

ER fractionation

ER fractionation protocols were adapted from Cox and Emili (2006)[22]. Briefly, male mice at three months of age (unless otherwise noted) with or without overnight fasting were anesthetized by tribromoethanol and perfused with 20ml 0.25M sucrose solution before tissue harvesting. Fresh liver tissue (1.0g for lean and 1.2g for obese mice produced an equal amount of ER) was immediately transferred to 10ml ice cold STM buffer (0.25M sucrose, 50mM Tris pH7.4, 5mM $MgCl_2$), chopped into small pieces and homogenized by 6 strokes in a motor-driven, loose-fit, teflon-glass homogenizer at speed setting of 3.5 (Wheaton, NJ). The whole lysates were first cleared by centrifugation at 3000g for 10 minutes followed by a series of centrifugations to obtain the final ER pellet. The pellet was washed with 11ml of ice-cold 0.25M sucrose solution and was subjected to

centrifugation to obtain the final ER preparation which was either snap frozen in liquid nitrogen or used directly for biochemical and other analysis.

Sample prefractionation by 1D-PAGE

20 µl (~100 µg) of the ER protein extract was boiled for 5 minutes in an equal volume of 2x Laemmli buffer and separated on a 12% SDS-poly-acrylamide gel (15 cm x 15 cm x 1.0 mm). The gel was minimally stained with Coomassie Brilliant Blue and briefly washed in 25% methanol, 7.5% acetic acid and sliced horizontally into 12 bands with roughly similar protein content as estimated from the optical density[25]. The gel was then cut vertically to separate the protein content of individual lanes. The gel slices were minced with a sterile clean razor blade, transferred into 96-well plates, washed three times with 200 µL of 25 mM ammonium bicarbonate 50% acetonitrile, followed by dehydration with 100 µL HPLC-grade acetonitrile. After removal of acetonitrile, the gel slices were dried completely in a vacuum concentrator (SpeedVac, Thermo, MA) and rehydrated in 200 µL of 50 mM ammonium bicarbonate containing 1 µg/ml trypsin, followed by incubation for 24 h at 37^0C. Protein digests were collected and the gel pieces were further extracted and washed a) with 200 µL of aqueous 20 mM ammonium bicarbonate pH 8.6; b) twice with 200 µL of 2% formic acid 50% HPLC-grade acetonitrile, followed by c) dehydration in 150 µL of 2% formic acid 10% 2-propanol 85% acetonitrile. The combined peptide solutions were filtered using hydrophilic multiwell PTFE filter plates (Millipore, MA) according to the manufacturer's protocol and concentrated to a volume of ~5 µL in a SpeedVac,

and resuspended in 60 µl aqueous solvent containing 2% formic acid, 2% acetonitrile. Samples were analyzed by 1D nano-LC ESI tandem mass spectrometry as described below.

Protein identification by 1D nano-LC tandem mass spectrometry

LC MS/MS instrumentation: A CTC Autosampler (LEAP Technologies, NC) was equipped with two 10-port Valco valves and a 20 µl injection loop. A 2D LC system (Eksigent, CA) was used to deliver the flow rate of 3 µl/min during sample loading and 250 nl/min during nanoflow rate LC separation. Self packed columns used: a C18 solid phase extraction "trapping" column (250 µm i.d. x 10 mm) and a nano-LC capillary column (100 µm i.d. x 15 cm, 8 µm i.d. pulled tip (NewObjective) both packed with the Magic C18AQ, 3 µm, 200 Å (Michrom Bioresources) stationary phase. A protein digest (10 µl) was injected onto the trapping column connected on-line with the nano-LC column through the 10-port Valco valve. The sample was cleaned up and concentrated using the trapping column, eluted onto and separated on the nano-LC column with a one-hour linear gradient of acetonitrile in 0.1% formic acid. The LC MS/MS solvents were Solvent A: 2% acetonitrile in aqueous 0.1% formic acid; and Solvent B: 5% isopropanol 85% acetonitrile in aqueous 0.1% formic acid. The 85-minute long LC gradient program included the following elution conditions: 2%B for 1 minute; 2-35%B in 60 minutes; 35-90%B in 10 minutes; 90%B for 2 minutes; and 90-2%B in 2 minutes. The eluent was introduced into LTQ Orbitrap (ThermoElectron, CA) mass spectrometer equipped with a nanoelectrospray source (New Objective,

MA) by nanoelectrospray. The source voltage was set to 2.2 kV and the temperature of the heated capillary was set to 180 ^{o}C. For each scan cycle on full MS scan was acquired in the Orbitrap mass analyzer at 60,000 mass resolution, 6x10^{5} AGC target and 1200 ms maximum ion accumulation time was followed by 7 MS/MS scans acquired for the 7 most intense ions for each of the following m/z ranges 350-700, 695-1200, and 1195-1700 amu. The LTQ mass analyzer was set for 30,000 AGC target and 100 ms maximum accumulation time, 2.2 Da isolation width, and 30 ms activation at 35% normalized collision energy. Dynamic exclusion was enabled for 45 s for each of the 200 ions that had been already selected for fragmentation to exclude them from repeated fragmentation. Each digest was analyzed twice.

MS data processing: The MS data .raw files acquired by the LTQ Orbitrap mass spectrometer were copied to the Sorcerer IDAII search engine (Sage-N Research, Thermo Electron, CA) and submitted for database searches using the SEQUEST-Sorcerer algorithm. The search was performed against a concatenated FASTA protein database containing the forward and reversed human (25H.Sapiens) UniProt KB database downloaded from EMBL-EBI on 10.23.2008 as well as an in-house compiled database with common contaminants. Methionine, histidine, and tryptophane oxidation (+15.994915 atomic mass units, amu) and cysteine alkylation (+57.021464 amu with iodoacetamide derivative) were set as differential modifications. No static modifications or differential posttranslational modifications were employed. A peptide mass tolerance equal to 30 ppm and a fragment ion mass tolerance

equal to 0.8 amu were used in all searches. Monoisotopic mass type, fully tryptic peptide termini, and up to 2 missed cleavages were used in all searches. The SEQUEST output was filtered, validated, and analyzed using Peptide Prophet, Protein Prophet (Institute for Systems Biology, WA) and Scaffold (Proteome Software, OR) software. The balance between reliability and sensitivity of the protein identification data was set by adjusting the estimated false positive peptide identification rate (FPR) to below 0.5%. The FPR was calculated as the number of peptide matches from a "reverse" database divided by the total number of "forward" protein matches, in percentages. The semiquantitative spectral count data sets obtained for all samples were subsequently integrated and processed using the in-house written software ProMerger which allowed us to compare proteomic profiles derived from different samples and perform the downstream pathway analysis.

Statistical methods of proteomic analysis

Spectral counts were computed for each protein in each sample by utilizing high quality MS/MS-based peptide identifications. In this study, we were primarily interested in detecting differentially abundant proteins between lean and obese mice, as opposed to absolute protein quantification or cross-protein comparisons of abundance, and we ultimately restricted our attention to proteins with average spectral count (across samples) greater than 5 for better reliability[26]. This obviates the need for certain within-protein normalization techniques[25,27,28]. To identify differentially abundant proteins, we fit a Poisson mixed model[29] for each protein. The Poisson mixed model allows for a principled treatment of discrete

count data and provides a statistically rigorous framework for the identification of differentially abundant proteins accounting for correlation among repeated measures and over-dispersion. A similar approach is followed in Choi et al.,[30]. However, our approach relies on fewer modeling assumptions than the Bayesian approach advocated by Choi et al., where variability of abundance is assumed to be constant across proteins -- a strong assumption that generally does not hold in practice. Our approach does not require this assumption. Because we rely on fewer modeling assumptions, it is reasonable to expect that our procedure is in fact more robust to model misspecification than Choi et al.'s.

The Poisson mixed model, unlike an ordinary Poisson model, accounts for over-dispersion often present in spectral count data. Indeed, to account for over-dispersion, we included a random intercept term for each mouse in the experiments. Furthermore, in order to adjust for difference in the overall protein abundance in each sample, we include an offset term depending on the total spectral counts (across all proteins) in each sample. Finally, even after including the offset term, we noticed substantial differences between the experiments, thus we controlled for an experiment effect in our analysis. In summary, for each protein, we fit the model described by the equation

$$\log(\mu_{ijk}) = \log(t_{ijk}) + \alpha + b_j + \gamma_k + \delta x_j,$$

where μ_{ijk} is the expected spectral count for the *i*-th technical replicate from the *j*-th mouse in experiment *k*, conditional on the mean zero mouse-specific random effect b_j; t_{ijk} is the total spectral counts in the sample; γ_k represents the *k*-th

experiment effect; and $x_j = 0$ or 1 according to whether the *j*-th mouse was from the lean or obese group and δ is the corresponding lean/obese effect. A total of five experiments were conducted. Each was comprised of four mice -- two lean and two obese samples. In one of the experiments, two samples per mouse were available (technical replicates), while in the other four experiments only a single sample per mouse was available. Thus, for each Poisson mixed model fit, a total of 24 observations were utilized. For us, the parameter of primary interest was δ. For each protein, we obtained a *p*-value corresponding to δ, and proteins were ranked by these *p*-values for significance. We used the R library lme4 to fit the Poisson mixed models.

Bioinformatic analysis of proteomics

Proteins identified as significantly up- or down-regulated in the obese ER proteome were analyzed by Database for Annotation, Visualization and Integrated Discovery (DAVID, http://david.abcc.ncifcrf.gov/)[31,32] and plotted in R. Clustering analysis was carried out with the Cluster3.0 program[33] and visualized either in JavaTreeview or MeV[33,34]. Functional annotation charts of proteins of interest (absolute median fold change ≥ 1.5, significance of fold change ≤ 0.05, average unadjusted spectral count of 5 across all experiments) were generated using the 'Biological Pathways' subset of Gene Ontology included in the DAVID System[38] using all identified ER proteins as the background set. Biological pathway annotations were manually curated to remove redundant (identical) annotations associated with the same sets of proteins.

Quantitative profiling of lipids and fatty acid compositions of ER and statistics

ER pellets (~50mg) were resuspended in 1ml of 0.25M sucrose, 200µl of which was used for lipid extraction in the presence of authentic internal standards by the method of Folch et al., with chloroform:methanol (2:1 v/v)[35]. Individual lipid classes were separated and quantified by liquid chromatography (Agilent Technologies model 1100 Series). To obtain the quantitative composition of fatty acids for each lipid class, the separated lipids were transesterified in 1% sulfuric acid/methanol at 100°C for 45 minutes and extracted by 0.05% butylated hydroxytoluene/hexane. The resulting fatty acid methyl esters were quantified by gas chromatography (Agilent Technologies model 6890) under nitrogen. The nmol% of each fatty acid was computed as the nmole quantity of the individual fatty acid divided by the total nmole amount of fatty acid isolated from each lipid class of each ER sample. The nmole% profile of fatty acids was then averaged in all six lean ER samples to examine the differences in the fatty acid profile that existed among different lipid classes. To identify compositional differences between control and experimental groups, Student's *t*-tests were performed for all fatty acid/lipid class combinations (26 x 9). The mean difference of nmol% for each fatty acid/lipid class combination with $p<0.05$ were visualized in MeV[34]. Complete cluster analyses were performed for the fatty acid compositions of control and experimental groups using the Cluster3.0 program[33] with the following filter setting: 100% present, at least 50% samples with nmole% ≥ 2 and (max-min) ≥ 1.

Calcium transport assays

The calcium transport assay for measuring Serca activity was adapted from Moore et al[23]. Briefly, fresh liver tissues were homogenized in 10 volumes of buffer containing 0.25M sucrose, 2mM Tris pH7.4 and 1mM DTT and EDTA-free protease inhibitor. The ER pellet was obtained after a series of centrifugation as described in the previous section, and then resuspended in 0.25M sucrose. The same procedure was employed to isolate microsomes from cultured Hepa1-6 cells except that cell pellet was lysed in hypotonic 0.1M sucrose, 2mM Tris pH7.4, 1mM DTT and EDTA-free protease inhibitor. The calcium transport assay was carried out in reaction buffer containing 0.1M KCl, 30mM, 5mM NaN_3, 5mM $MgCl_2$, 5mM $K_2C_2O_4$, 50μM of $CaCl_2$ (plus 1μCi/μmol of ^{45}Ca), 1μM Rethenium Red, 5mM ATP. The reaction was started by the addition of microsomes containing 150μg proteins for 15 minutes in a 37ºC water bath and stopped by the addition of 0.15M KCl, 1mM $LaCl_3$ and filtered through a 0.2μ HT Tuffryn membrane (PALL Corporation, NY). The calcium transport experiment with lipid overloading was carried out essentially as previously described[5] except that liposomes were made of egg derived PC and PE by the ethanol injection method[36]. The amount of SERCA independent calcium transport was quantified in the presence of 10μM thapsigargin and subtracted from the calculation.

Western blotting, real-time quantitative PCR and molecular cloning

For the preparation of total cellular proteins, ~0.1g of liver tissues were homogenized in 1ml of a cold lysis buffer containing 50 mM Tris-HCl (pH 7.0), 2

mM EGTA, 5 mM EDTA, 30 mM NaF, 10 mM Na_3VO_4, 10 mM $Na_4P_2O_7$, 40 mM β-glycerophosphate, 1% NP-40, and 1% protease inhibitor cocktail. After a brief centrifugation (200g x 10 minutes) to pellet down cell debris, 1/5 volume of 6x Laemmli buffer was added into the whole cell lysate, boiled and centrifuged at 10,000g for 10 minutes. Protein concentrations were quantified with Bio-Rad D_c Protein Assay (Bio-Rad, CA). Western blotting of protein of interest was done as previously described[4,10]. Total RNA was extracted with Trizol reagent according to manufacturer's recommendations. A total of 2μg of RNA was used for cDNA synthesis using High Capacity cDNA archiving system (Applied Biosystems). The SYBR real-time PCR system was used to quantify the transcript abundance for genes of interest (Supplemental Table S6). Either 18S or 28S rRNA was used for internal control.

Adenovirus-mediated loss- or gain-of-function experiments

For *Pemt* knockdown experiments, a series of DNA hairpins specifically targeting the mouse *Pemt* gene were designed by RNAxs (http://rna.tbi.univie.ac.at/cgi-bin/RNAxs)[37], synthesized, cloned into the **pENTR/U6** system (Invitrogen, CA) and tested in the Hepa1-6 cell line. The sequence with best efficacy, and it has 5nt mismatch with the next closest match of genes, were recloned into the **pAD/Block-iT-DEST** system through recombination, as described[24]. The *LacZ* shRNA was also cloned into the **pAD/Block-iT-DEST** system as control. For *Serca2b* over-expression experiment, the open reading frame of human *Serca2b* or *Gfp* (control) was amplified, cloned into **pENTR/TOPO** vector and then

recombined into the **pAD/CMV/V5-DEST** vector. Adenovirus (serotype 5, Ad5) for the construct of interest was produced and amplified in 293A cells, purified using CsCl column, desalted, and $1x10^{11}$ virus particles were used for each injection. Adenovirus transductions of mice were performed between 10-11 weeks of age. Blood glucose levels were measured after 6 hours of food withdrawal (9am-3pm) at before and 5 days post-injection and at the time of harvest (9-12 days). For histological analysis, liver tissues were fixed in 10% formalin solution, and sectioned for Hematoxylin and Eosin staining. All oligonucleotide sequences are listed in the Supplementary Table 6.

SUPPLEMENTARY FIGURE LEGENDS

Supplementary Figure 1: ER fractionation and validation.

a, Illustration of ER fractionation procedure for proteomic and lipidomic analyses and polysome profiling. **b,** Validation of ER fractionation methodology by immunoblot analyses of subcellular markers. PDI: protein disulfide isomerase, CANX: Calnexin, IR: Insulin receptor, H2A: Histone 2A**. c,** Volcano plot of the fold changes of median spectral counts of proteins from obese and lean samples against the significance of differential expression (log-normalized p-Values). Proteins of interest are highlighted (red: $p<0.05$, fold of change (obese/lean) ≥1.5, average spectral counts ≥ 5; green: $p<0.05$, fold of change (lean/obese) ≥ 1.5, average spectral counts ≥ 5). **d,** Immunoblot of differentially regulated proteins identified from the proteomic study for protein lysates prepared from cytosolic and ER fractions of unfasted lean and obese liver. PMSA: Proteasome small subunit a, RPS6: Ribosomal small subunit 6, APOB: Apolipoprotein B, Mtp: Microsmal triglyceride transfer protein, HP: Hepatoglobin, ASGR: Asialoglycoprotein receptor, mEH: Microsomal epoxide hydrolase, MRC1: Mannose receptor, C type 1.

Supplementary Figure 2: Expression of ER stress markers in the obese liver.

a, Immunoblot detection of representative ER stress markers in total protein lysates prepared from the liver of lean and ob/ob mice sacrificed at 12 weeks of age after 6 hours of food withdrawal. **b**, Transcript levels of genes involved in

ER-associated protein degradation (ERAD) in the liver of lean and ob/ob mice as determined by quantitative RT-PCR.

Supplementary Figure 3: Distinct contributions of dietary fat and *de novo* lipogenesis to ER lipid composition.

a, Illustration of the synthesis of nine classes of lipids detected in the ER lipidome. Dashed lines indicate multiple enzymetic steps. Genes studied herein are colored red. **b,** Heatmap display of all significant (p<0.05, Student's t-test) alterations present between diet and lean ER lipidomes. The color scheme reflects differences calculated based on the relative abundance (nmol%) of each fatty acid among individual lipid groups detected in the ER of lean liver and the diet. **c,** Complete linkage analysis of all twelve ER lipidomes (6 lean vs 6 obese). The length of each branch correlates with the magnitude of lipidomic differences.

Supplementary Figure 4: The effect of *Pemt* knockdown on liver ER lipidome and ER stress in ob/ob mice.

a, Transcript levels of *Pemt* in the liver of ob/ob mice administered with adenoviral control (*LacZ* shRNA) or *Pemt* shRNA expressing viruses. **b,** Heatmap display of the fatty acid composition of ER isolated from the liver of ob/ob mice administered with control and *Pemt* shRNA. The color scheme denotes differences calculated from the relative abundance (nmol%) of each fatty acid among individual lipid groups detected in the ER of control and *Pemt* shRNA liver samples. **c,** Complete linkage analysis of ER lipidome for samples prepared from control and experimental groups. **d,** Quantification of immunoblot signals

presented in Figure 3d. Values are mean±SEM, n=4, "*" denotes $p<0.05$, Student's *t*-test.

Supplementary Figure 5: Amelioration of ER stress in the liver of high-fat diet (HFD) induced obese mouse by *Pemt* knockdown.

a-b, Hematoxylin & Eosin staining of liver sections prepared from control (**a**) as well as *Pemt* shRNA-treated mice after 22 weeks of HFD (**b**). The white vesicles represent lipid droplets. **c,** Blood glucose levels of control and *Pemt* shRNA-treated HFD mice. **d-e,** Immunoblot and quantification of ER stress markers in the liver of control and experimental HFD mice. Values are mean±SEM, n=4, "*" denotes $p<0.05$, Student's *t*-test.

Supplementary Figure 6: SERCA2b overexpression improves systematic glucose homeostasis of ob/ob mice.

Plasma glucose levels of control and SERCA2b overexpressing ob/ob mice after intraperitoneal administration of either 1IU/kg of insulin (**a**) or 1g/kg of glucose (**b**). All data are mean±SEM, "*" denotes $p<0.05$ (one-way ANOVA, n=6/group).

Supplementary Figure 7: Detergent-dependent solubilization of SERCA2b proteins from fatty liver samples and comparison of SERCA2b expression in lean and obese animals.

a, Immunoblot of total protein lysates as well as ER fractions prepared from the liver of lean and obese mice following two different solubilization methods from the same samples. Liver tissue was first homogenized in lysis buffer containing

1% NP40 and clarified at 200g for 10 minutes to pellet down cell debris. The whole cell lysate was either further solubilized by the addition of Laemmli buffer (2% SDS, top panel) or clarified by consecutive centrifugations at 16,000g for 10 minutes and 60 minutes (middle panel) as described in Park et al., (2010)[16], supernatant collected, boiled in Laemmli buffer and loaded on to SDS-PAGE. For the examination of SERCA2b protein levels in the liver ER (bottom panel), ER pellet was resuspended in Laemmli buffer (2% SDS), sonicated for 3 minutes, boiled and clarified by centrifugation at 10,000g for 10 minutes. **b-c**, Transcript levels of *Serca2b* in the liver tissues of genetically obese (12 weeks old, **b**) and diet-induced obese (22 weeks of HFD) mice as compared to age-matched lean controls. **d**-**e**, SERCA2b protein levels in the liver tissues of genetically obese as well as diet-induced obese mice at different ages. The total protein lysates were prepared with Laemmli buffer containing 2% SDS as described in the Methods.

SUPPLEMENTAL REFERENCES

25. Schmidt, M. W., Houseman, A., Ivanov, A. R., and Wolf, D. A., Comparative proteomic and transcriptomic profiling of the fission yeast Schizosaccharomyces pombe. *Mol Syst Biol* **3**, 79 (2007).

26. Liu, H., Sadygov, R. G., and Yates, J. R., 3rd, A model for random sampling and estimation of relative protein abundance in shotgun proteomics. *Anal Chem* **76** (14), 4193 (2004).

27. Ishihama, Y. et al., Exponentially modified protein abundance index (emPAI) for estimation of absolute protein amount in proteomics by the number of sequenced peptides per protein. *Mol Cell Proteomics* **4** (9), 1265 (2005).

28. Lu, P. et al., Absolute protein expression profiling estimates the relative contributions of transcriptional and translational regulation. *Nat Biotechnol* **25** (1), 117 (2007).

29. Diggle, P. J., Heagerty, P., Liang, K.-Y., and Zeger, S. L. , in *Analysis of Longitudinal Data.* (Oxford Press, 2002).

30. Choi, H., Fermin, D., and Nesvizhskii, A. I., Significance analysis of spectral count data in label-free shotgun proteomics. *Mol Cell Proteomics* **7** (12), 2373 (2008).

31. Dennis, G., Jr. et al., DAVID: Database for Annotation, Visualization, and Integrated Discovery. *Genome Biol* **4** (5), P3 (2003).

32. Huang, D.W., Sherman, B. T., and Lempicki, R. A., Systematic and integrative analysis of large gene lists using DAVID bioinformatics resources. *Nat Protoc* **4** (1), 44 (2009).

33. Eisen, M. B., Spellman, P. T., Brown, P. O., and Botstein, D., Cluster analysis and display of genome-wide expression patterns. *Proc Natl Acad Sci U S A* **95** (25), 14863 (1998).

34. Saeed, A. I. et al., TM4 microarray software suite. *Methods Enzymol* **411**, 134 (2006).

35. Folch, J., Lees, M., and Sloane Stanley, G. H., A simple method for the isolation and purification of total lipides from animal tissues. *J Biol Chem* **226** (1), 497 (1957).

36. Watanabe, J., Asaka, Y., Mino, K., and Kanamura, S., Preparation of liposomes that mimic the membrane of endoplasmic reticulum of rat hepatocytes. *J Electron Microsc (Tokyo)* **45** (2), 171 (1996).

37. Tafer, H. et al., The impact of target site accessibility on the design of effective siRNAs. *Nat Biotechnol* **26** (5), 578 (2008).

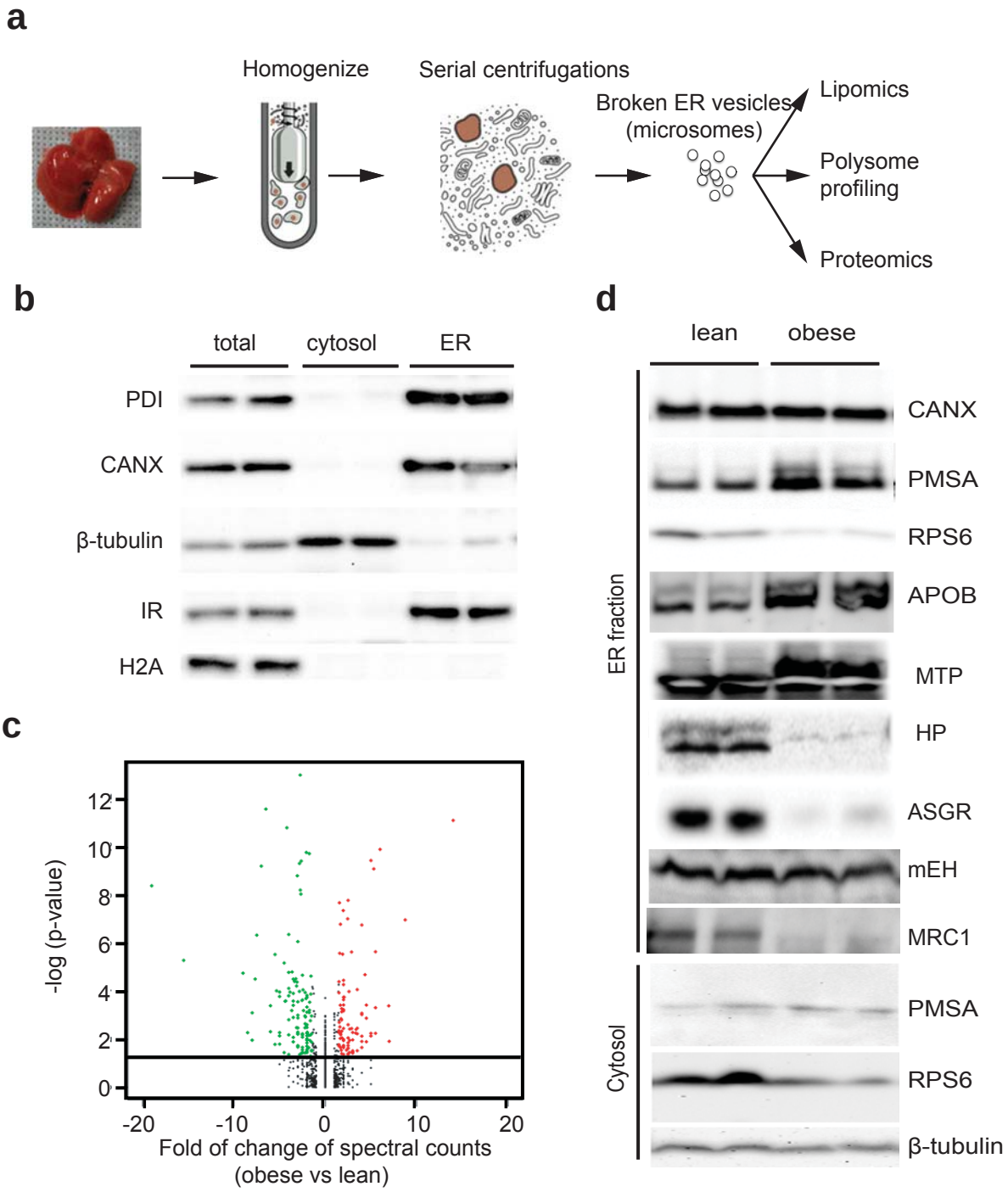

Supplementary Figure 1

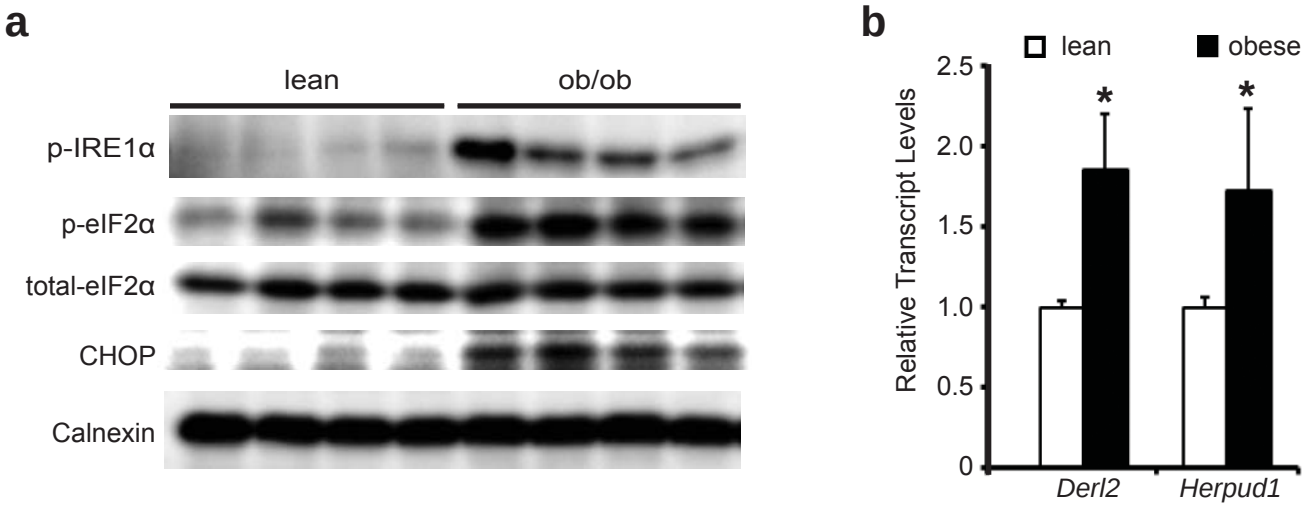

Supplementary Figure 2

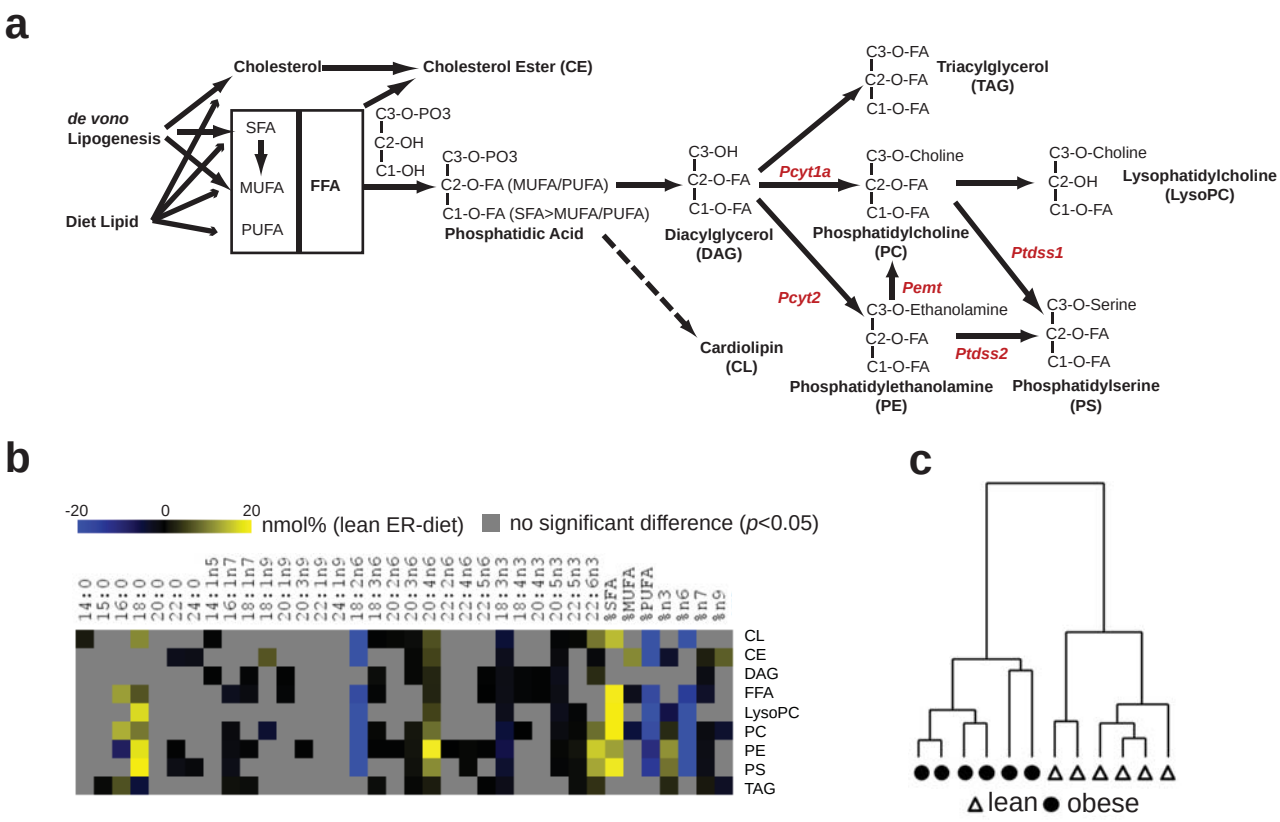

Supplementary Figure 3

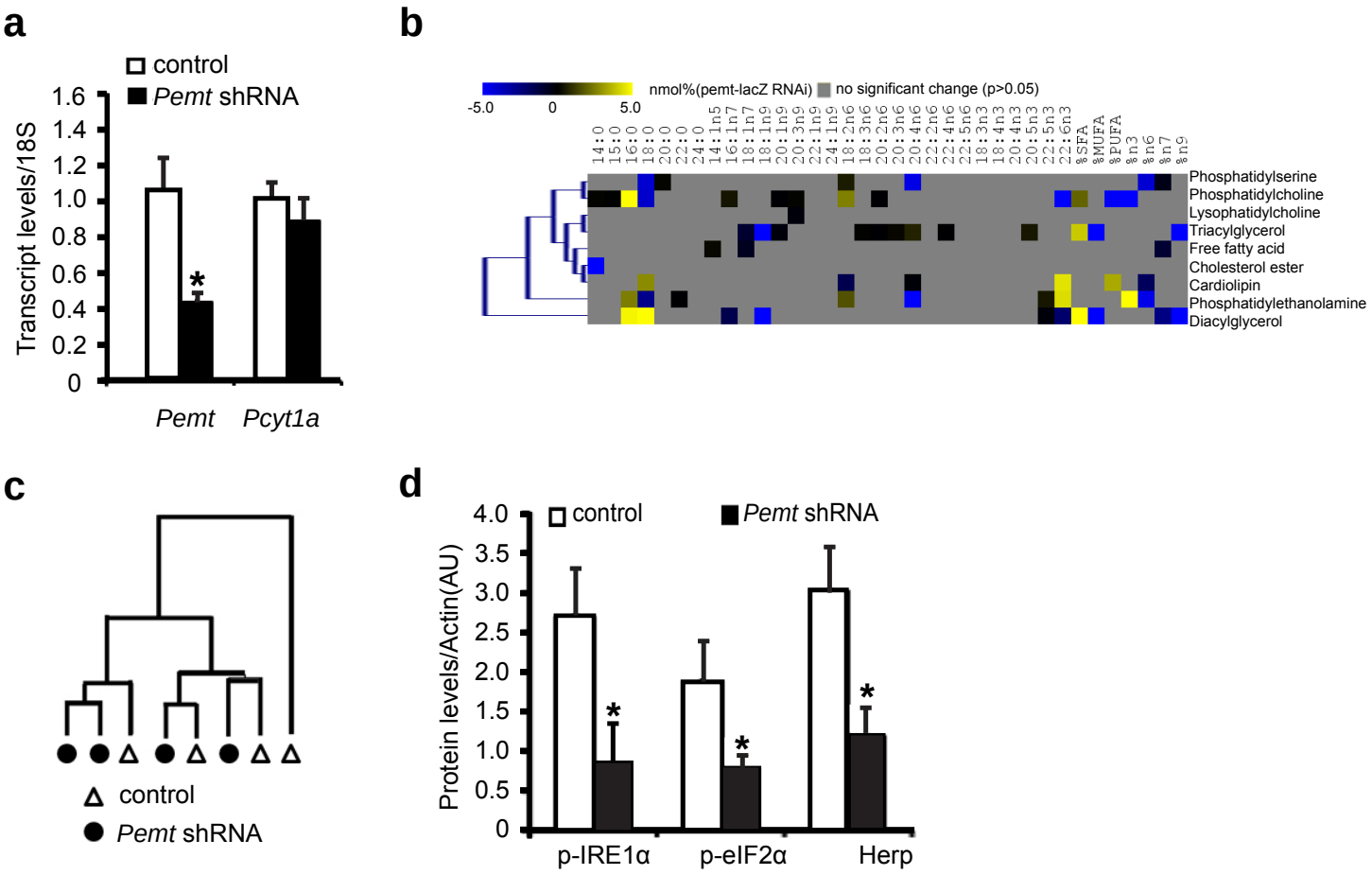

Supplementary Figure 4

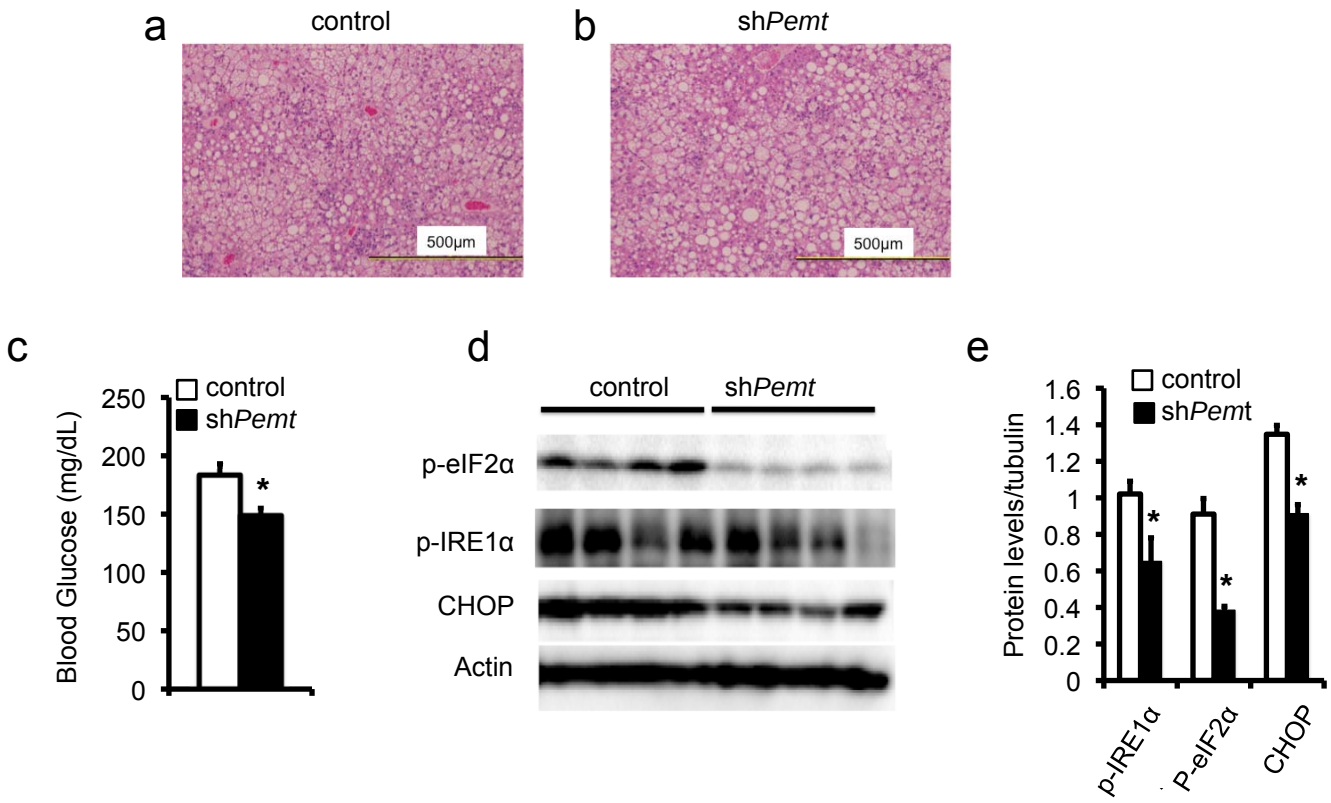

Supplementary Figure 5

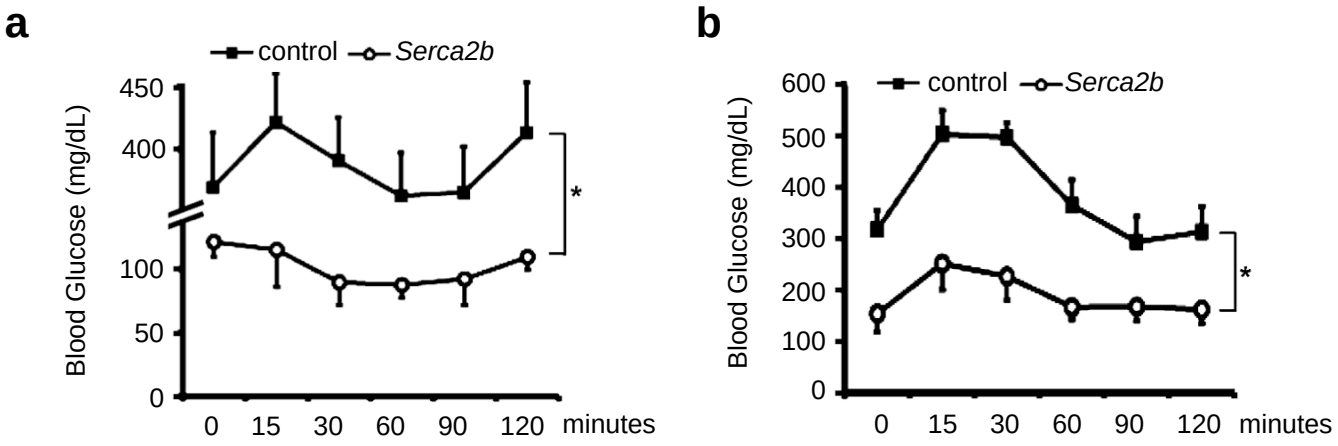

Supplementary Figure 6

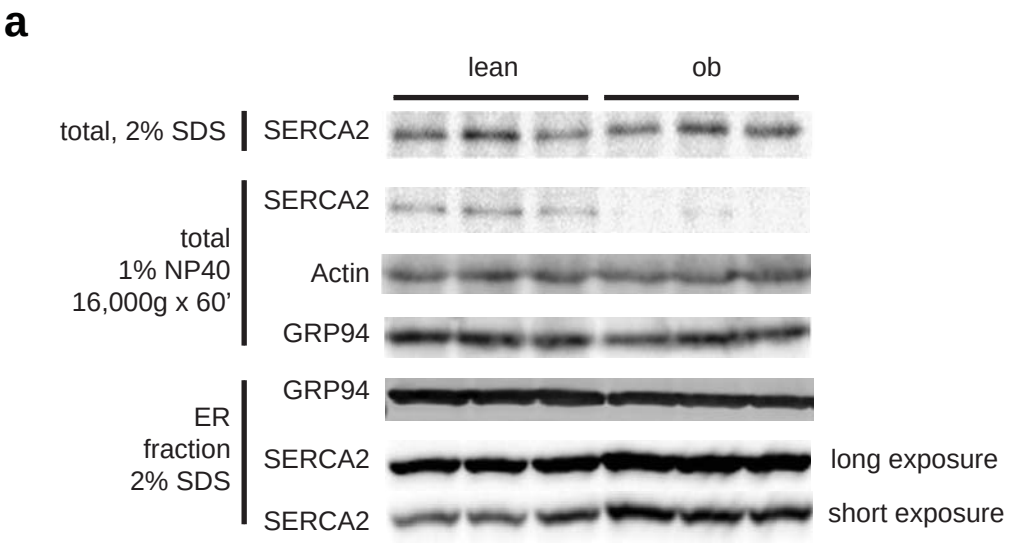

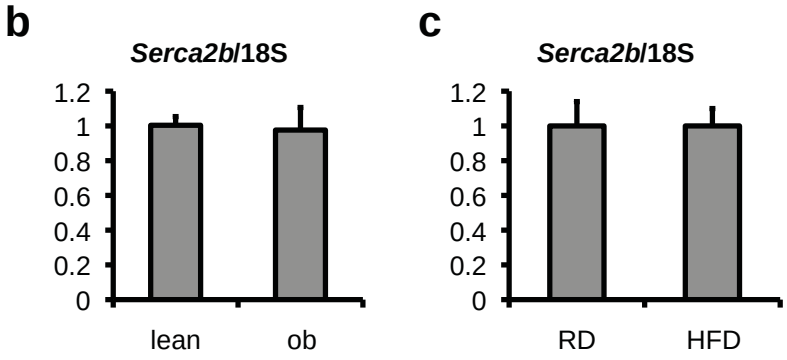

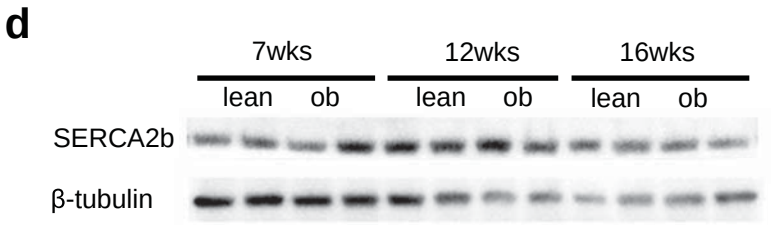

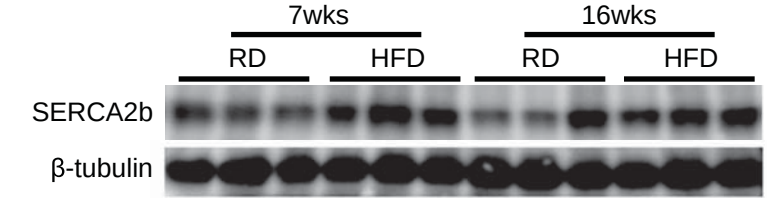

Supplementary Figure 7

Supplementary Table 2a. The Up-regulated Proteins in the Obese Liver ER Proteome.

Symbol	UniProt Accession	MW(kDa)	Nomenclature	Fold Change	p.val
Acaa1b	Q8VCH0|THIKB_MOUSE	44	acetyl-Coenzyme A acyltransferase 1B	14.0	7.37E-12
Fasn	P19096|FAS_MOUSE	272	fatty acid synthase	8.8	1.04E-07
Oplah	Q8K010|OPLA_MOUSE	138	5-oxoprolinase (ATP-hydrolysing)	7.0	1.21E-02
Pcx	Q3T9S7|Q3T9S7_MOUSE	130	pyruvate carboxylase	7.0	4.00E-04
Apoa4	P06728|APOA4_MOUSE	45	apolipoprotein A-IV	6.0	1.19E-10
Pklr	P53657|KPYR_MOUSE	62	pyruvate kinase liver and red blood cell	5.5	2.22E-06
Aldh3a2	Q5SRE0|Q5SRE0_MOUSE	59	aldehyde dehydrogenase family 3, subfamily A2	5.3	7.74E-10
Tuba1a	P68369|TBA1A_MOUSE	50	tubulin, alpha 1A	5.0	7.22E-03
Tubb2b	Q9CWF2|TBB2B_MOUSE	50	tubulin, beta 2B	5.0	3.46E-10
Gpd1	P13707|GPDA_MOUSE	38	glycerol-3-phosphate dehydrogenase 1 (soluble)	4.5	3.71E-04
Acaca	Q5SWU9|COA1_MOUSE	265	acetyl-Coenzyme A carboxylase alpha	4.3	2.01E-05
Psmd1	Q3TXS7|PSMD1_MOUSE	106	proteasome (prosome, macropain) 26S subunit, non-ATPase, 1	4.0	2.19E-02
Myh14	Q6URW6|MYH14_MOUSE	229	myosin, heavy polypeptide 14	4.0	9.25E-04
Eno1	P17182|ENOA_MOUSE	47	enolase 1, alpha non-neuron	4.0	1.70E-07
Mylc2b	Q3THE2|MLRB_MOUSE	20	myosin, light chain 12B, regulatory	3.4	3.83E-03
Ugp2	Q91ZJ5|UGPA_MOUSE	57	UDP-glucose pyrophosphorylase 2	3.3	5.47E-03
Coasy	Q9DBL7|COASY_MOUSE	62	Coenzyme A synthase	3.0	1.05E-02
Ces3	Q8VCT4|CES3_MOUSE	62	carboxylesterase 3	2.9	3.53E-03
Gstm1	A2AE89|A2AE89_MOUSE	24	glutathione S-transferase, mu 1	2.9	2.27E-06
Pygl	Q9ET01|PYGL_MOUSE	97	liver glycogen phosphorylase	2.7	3.69E-03
Hbb-b1	A8DUK7|A8DUK7_MOUSE	16	hemoglobin, beta adult major chain	2.6	3.52E-02
Dak	Q8VC30|DAK_MOUSE	60	dihydroxyacetone kinase 2 homolog (yeast)	2.6	1.01E-04
Fmo1	P50285|FMO1_MOUSE	60	flavin containing monooxygenase 1	2.5	1.39E-02
Aldob	Q91Y97|ALDOB_MOUSE	40	aldolase B, fructose-bisphosphate	2.5	9.39E-08
Cat	P24270|CATA_MOUSE	60	catalase	2.3	2.81E-02
P4hb	P09103|PDIA1_MOUSE	57	prolyl 4-hydroxylase, beta polypeptide	2.1	1.73E-04
Sds	Q8VBT2|SDHL_MOUSE	35	serine dehydratase	2.0	1.79E-02
Gstz1	Q9JJA0|Q9JJA0_MOUSE	16	glutathione transferase zeta 1 (maleylacetoacetate isomerase)	2.0	3.45E-05
Ephx1	P97869|P97869_MOUSE	53	epoxide hydrolase 1, microsomal	2.0	4.24E-08
Maob	Q8BW75|AOFB_MOUSE	59	monoamine oxidase B	1.9	2.80E-06
Cyb5r3	Q9CY59|Q9CY59_MOUSE	34	cytochrome b5 reductase 3	1.8	8.66E-03
Trf	Q921I1|TRFE_MOUSE	77	transferrin	1.8	4.52E-03
Cyb5	P56395|CYB5_MOUSE	15	cytochrome b-5	1.8	3.97E-02
Acsl5	Q8JZR0|ACSL5_MOUSE	76	acyl-CoA synthetase long-chain family member 5	1.8	1.55E-03
Phb	P67778|PHB_MOUSE	30	prohibitin	1.8	2.86E-02
Aldh1a1	P24549|AL1A1_MOUSE	54	aldehyde dehydrogenase family 1, subfamily A1	1.7	1.38E-03
Slc25a5	P51881|ADT2_MOUSE	33	solute carrier family 25 (mitochondrial carrier, adenine nucleotide translocator), member 5	1.7	6.42E-03
Atp5h	Q9DCX2|ATP5H_MOUSE	19	ATP synthase, H+ transporting, mitochondrial F0 complex, subunit d	1.7	2.23E-02
Mttp	O08601|MTP_MOUSE	99	microsomal triglyceride transfer protein	1.7	5.71E-03
Atp5a1	Q03265|ATPA_MOUSE	60	ATP synthase, H+ transporting, mitochondrial F1 complex, alpha subunit, isoform 1	1.7	1.58E-07
Fmo5	P97872|FMO5_MOUSE	60	flavin containing monooxygenase 5	1.7	3.75E-04
Atp5o	Q9DB20|ATPO_MOUSE	23	ATP synthase, H+ transporting, mitochondrial F1 complex, O subunit	1.6	9.15E-03
Etfdh	Q6PF96|Q6PF96_MOUSE	61	electron transferring flavoprotein, dehydrogenase	1.6	3.01E-03
Mvp	Q3THX5|Q3THX5_MOUSE	97	major vault protein	1.6	2.57E-06
Apoe	P08226|APOE_MOUSE	36	apolipoprotein E	1.6	2.01E-08
Mat1a	Q91X83|METK1_MOUSE	44	methionine adenosyltransferase I, alpha	1.5	1.95E-03
Gapdh	P16858|G3P_MOUSE	36	glyceraldehyde-3-phosphate dehydrogenase	1.5	1.90E-02
Rps13	P62301|RS13_MOUSE	17	ribosomal protein S13	1.5	1.67E-02
Flnb	Q80X90|FLNB_MOUSE	278	filamin, beta	1.5	4.31E-03
Myl6	Q60605|MYL6_MOUSE	17	myosin, light polypeptide 6, alkali, smooth muscle and non-muscle	1.5	5.16E-03

Supplementary Table 2b. The Down-regulated Proteins in the Obese Liver ER Proteome.

Symbol	UniProt Accession	MW(kDa)	Nomenclature	Fold Change	p.val
Gne	A2AJ63|A2AJ63_MOUSE	11	glucosamine	-19.0	3.92E-09
Eif3f	Q9DCH4|EIF3F_MOUSE	38	eukaryotic translation initiation factor 3, subunit F	-15.5	5.07E-06
Eif2s2	Q99L45|IF2B_MOUSE	38	eukaryotic translation initiation factor 2, subunit 2 (beta)	-8.5	5.25E-03
Eef1g	Q9D8N0|EF1G_MOUSE	50	eukaryotic translation elongation factor 1 gamma	-8.0	1.08E-02
Eif3g	Q9Z1D1|EIF3G_MOUSE	36	eukaryotic translation initiation factor 3, subunit G	-8.0	7.80E-04
Eif2s3x	A2AAW9|A2AAW9_MOUSE	37	eukaryotic translation initiation factor 2, subunit 3, structural gene X-linked	-7.7	3.06E-05
Egfr	Q01279|EGFR_MOUSE	135	epidermal growth factor receptor	-6.5	2.48E-12
Tdo2	P48776|T23O_MOUSE	48	tryptophan 2,3-dioxygenase	-6.0	3.96E-04
Pfkfb1	P70266|F261_MOUSE	55	6-phosphofructo-2-kinase/fructose-2,6-biphosphatase 1	-6.0	4.79E-03
Sept9	A2A6U3|A2A6U3_MOUSE	64	septin 9	-5.5	1.62E-02
Eif3e	P60229|EIF3E_MOUSE	52	eukaryotic translation initiation factor 3, subunit E	-5.3	9.44E-05
Eif3m	Q3TI04|Q3TI04_MOUSE	43	eukaryotic translation initiation factor 3, subunit M	-5.0	1.63E-04
Prps1	Q3TI27|Q3TI27_MOUSE	35	phosphoribosyl pyrophosphate synthetase 1	-4.5	3.57E-02
Mrc1	Q61830|MRC1_MOUSE	165	mannose receptor, C type 1	-4.4	2.57E-04
Atp11c	Q9QZW0|AT11C_MOUSE	129	ATPase, class VI, type 11C	-4.2	1.49E-11
Gcn1l1	Q3U3Z4|Q3U3Z4_MOUSE	118	GCN1 general control of amino-acid synthesis 1-like 1 (yeast)	-4.0	1.52E-03
Eif2s1	Q6ZWX6|IF2A_MOUSE	36	eukaryotic translation initiation factor 2, subunit 1 alpha	-3.9	1.07E-04
Eif4b	Q8BGD9|IF4B_MOUSE	69	eukaryotic translation initiation factor 4B	-3.7	6.28E-04
Gstp1	P19157|GSTP1_MOUSE	24	glutathione S-transferase, pi 1	-3.6	1.54E-05
Eif3c	Q8R1B4|EIF3C_MOUSE	106	eukaryotic translation initiation factor 3, subunit C	-3.4	3.84E-05
Dnm2	P39054|DYN2_MOUSE	98	dynamin 2	-3.2	2.97E-05
Eif3h	Q8BMZ8|Q8BMZ8_MOUSE	7	eukaryotic translation initiation factor 3, subunit H	-3.1	5.95E-05
Eif3i	Q9QZD9|EIF3I_MOUSE	36	eukaryotic translation initiation factor 3, subunit I	-3.1	3.24E-03
Eif3d	O70194|EIF3D_MOUSE	64	eukaryotic translation initiation factor 3, subunit D	-3.1	4.08E-05
Eif3b	Q8CIJ3|Q8CIJ3_MOUSE	109	eukaryotic translation initiation factor 3, subunit B	-3.1	1.50E-09
Actr1b	Q8R5C5|ACTY_MOUSE	42	ARP1 actin-related protein 1 homolog B, centractin beta (yeast)	-3.0	1.89E-02
Cad	Q6P9L1|Q6P9L1_MOUSE	158	carbamoyl-phosphate synthetase 2, aspartate transcarbamylase, and dihydroorotase	-3.0	9.82E-04
Abce1	P61222|ABCE1_MOUSE	67	ATP-binding cassette, sub-family E (OABP), member 1	-2.8	1.00E-04
Eif3eip	Q8QZY1|IF3EI_MOUSE	67	eukaryotic translation initiation factor 3, subunit L	-2.8	4.61E-10
Lman1	Q3U944|Q3U944_MOUSE	61	lectin, mannose-binding, 1	-2.8	4.30E-02
Asgr1	P34927|ASGR1_MOUSE	33	asialoglycoprotein receptor 1	-2.7	9.43E-14
Lrp1	Q91ZX7|LRP1_MOUSE	505	low density lipoprotein receptor-related protein 1	-2.7	5.92E-09
Usp9x	A2AD18|A2AD18_MOUSE	291	ubiquitin specific peptidase 9, X chromosome	-2.7	3.96E-02
Eif3a	P23116|EIF3A_MOUSE	162	eukaryotic translation initiation factor 3, subunit A	-2.7	8.68E-09
Scamp3	Q3TDM8|Q3TDM8_MOUSE	35	secretory carrier membrane protein 3	-2.6	3.64E-10
Rps8	P62242|RS8_MOUSE	24	ribosomal protein S8	-2.5	2.38E-04
Cyp2c50	Q91X77|CY250_MOUSE	56	cytochrome P450, family 2, subfamily c, polypeptide 50	-2.5	6.51E-03
Rrbp1	A2AVJ7|A2AVJ7_MOUSE	158	ribosome binding protein 1	-2.5	5.84E-03
Eif3j	Q3UGC7|Q3UGC7_MOUSE	29	eukaryotic translation initiation factor 3, subunit J	-2.4	8.60E-05
Hpx	Q3UKP2|Q3UKP2_MOUSE	51	hemopexin	-2.4	6.30E-04
Atl2	Q6PA06|ATLA2_MOUSE	66	atlastin GTPase 2	-2.2	3.28E-03
Cyp2d9	P11714|CP2D9_MOUSE	57	cytochrome P450, family 2, subfamily d, polypeptide 9	-2.2	3.68E-02
Copb1	Q9JIF7|COPB_MOUSE	107	coatomer protein complex, subunit beta 1	-2.2	1.05E-03
Vps26a	P40336|VP26A_MOUSE	38	vacuolar protein sorting 26 homolog A (yeast)	-2.2	1.11E-04
Ccdc22	Q9JIG7|CCD22_MOUSE	71	coiled-coil domain containing 22	-2.2	2.23E-03
Ugt2b1	Q8R084|Q8R084_MOUSE	60	UDP glucuronosyltransferase 2 family, polypeptide B1	-2.2	1.16E-03
Copa	Q8BTF0|Q8BTF0_MOUSE	139	coatomer protein complex subunit alpha	-2.1	1.98E-04
Pigr	O70570|PIGR_MOUSE	85	polymeric immunoglobulin receptor	-2.1	1.60E-10
Cyp1a2	P00186|CP1A2_MOUSE	58	cytochrome P450, family 1, subfamily a, polypeptide 2	-2.1	2.53E-03
Cct3	P80318|TCPG_MOUSE	61	chaperonin containing Tcp1, subunit 3 (gamma)	-2.0	1.96E-02
Gnb2l1	P68040|GBLP_MOUSE	35	guanine nucleotide binding protein (G protein), beta polypeptide 2 like 1	-2.0	1.41E-02
Dpp4	P28843|DPP4_MOUSE	87	dipeptidylpeptidase 4	-2.0	5.62E-03
Mup12	A2CEK7|A2CEK7_MOUSE	21	major urinary protein 12	-2.0	1.01E-02
Hp	Q61646|HPT_MOUSE	39	haptoglobin	-2.0	4.50E-04
M6pr	P24668|MPRD_MOUSE	31	mannose-6-phosphate receptor, cation dependent	-2.0	3.18E-03
Ap1m1	P35585|AP1M1_MOUSE	49	adaptor-related protein complex AP-1, mu subunit 1	-2.0	2.44E-03
Eif4a1	P60843|IF4A1_MOUSE	46	eukaryotic translation initiation factor 4A1	-2.0	5.05E-03
Abca6	Q8K441|ABCA6_MOUSE	183	ATP-binding cassette, sub-family A (ABC1), member 6	-1.8	6.82E-03
Anxa11	P97384|ANX11_MOUSE	54	annexin A11	-1.8	2.23E-02
Igf2r	Q07113|MPRI_MOUSE	274	insulin-like growth factor 2 receptor	-1.8	7.61E-04
Cpne3	Q8BT60|CPNE3_MOUSE	60	copine III	-1.8	1.79E-10
Vps35	Q9EQH3|VPS35_MOUSE	92	vacuolar protein sorting 35	-1.7	6.09E-04
Clint1	Q3UGL3|Q3UGL3_MOUSE	68	clathrin interactor 1	-1.7	2.82E-04
Cope	O89079|COPE_MOUSE	35	coatomer protein complex, subunit epsilon	-1.7	1.11E-02
Dnaja1	P63037|DNJA1_MOUSE	45	DnaJ (Hsp40) homolog, subfamily A, member 1	-1.6	1.66E-03
Rps6	P62754|RS6_MOUSE	29	ribosomal protein S6	-1.6	1.29E-04
Rdh7	O88451|RDH7_MOUSE	36	retinol dehydrogenase 7	-1.6	2.30E-05
Arcn1	Q3U4S9|Q3U4S9_MOUSE	57	archain 1	-1.5	2.85E-02
Aadac	Q99PG0|AAAD_MOUSE	45	arylacetamide deacetylase (esterase)	-1.5	2.90E-02
Ugt2b5	P17717|UD2B5_MOUSE	61	UDP glucuronosyltransferase 2 family, polypeptide B5	-1.5	5.89E-03

Supplementary Table 3. Lipid Composition of Endoplasmic Reticulum Prepared from Obese and Lean Mouse Liver Tissues

Lipid Class(nmol%)	ob#1	ob#2	ob#3	ob#4	ob#5	ob#6	lean#1	lean#2	lean#3	lean#4	lean#5	lean#6	diet#1	diet#2	ob.ave	lean.ave	TTEST
Cholesterol Ester	4.071	8.442	1.183	1.691	2.442	1.381	1.488	3.490	6.031	5.883	4.367	1.354	0.010	0.010	3.201	3.769	0.696
Diacylglycerol	5.617	3.476	1.982	3.470	4.269	1.968	1.454	2.557	3.577	4.269	1.442	2.468	0.038	0.037	3.464	2.628	0.281
Free cholesterol	17.245	18.869	10.058	15.920	21.385	7.233	9.494	9.155	13.603	18.338	11.266	9.528	0.118	0.121	15.118	11.897	0.251
Free fatty acid	8.286	10.921	5.763	10.017	5.356	8.776	5.295	8.452	20.915	12.701	6.277	7.163	0.006	0.005	8.187	10.133	0.466
Triacylglycerol	12.320	9.442	11.248	6.651	11.386	9.335	9.986	10.135	5.945	7.998	9.592	11.400	0.733	0.732	10.064	9.176	0.456
Phospholipids	52.461	48.849	69.767	62.251	55.161	71.308	72.283	66.212	49.930	50.813	67.056	68.065	0.095	0.095	59.966	62.393	0.665
Cardiolipin	4.994	3.331	2.680	2.974	3.263	2.711	4.543	3.237	4.469	3.471	3.590	3.779	0.032	0.031	3.326	3.848	0.237
Lysophosphatidylcholine	3.272	4.599	1.776	3.366	3.960	2.014	2.923	1.488	3.953	6.940	2.102	1.529	0.011	0.011	3.164	3.156	0.993
Phosphatidylcholine	26.088	21.077	38.680	36.270	26.469	41.815	31.917	33.044	20.967	17.553	31.225	32.340	0.027	0.026	31.733	27.841	0.394
Phosphatidylethanolamii	12.230	12.416	22.146	13.846	16.444	20.947	27.409	24.159	13.067	15.011	25.292	25.826	0.019	0.021	16.338	21.794	0.105
Phosphatidylserine	5.876	7.426	4.485	5.795	5.025	3.820	5.491	4.284	7.474	7.838	4.847	4.592	0.006	0.006	5.404	5.754	0.675
PC/PE	2.133	1.698	1.747	2.620	1.610	1.996	1.164	1.368	1.605	1.169	1.235	1.252	1.389	1.229	1.967	1.299	**0.003**
PC/PS	2.081	1.672	4.938	2.389	3.273	5.483	4.992	5.639	1.748	1.915	5.218	5.624	4.195	4.446	3.306	4.189	0.393

Supplementary Table 4. The ER Lipid Composition of Obese Mouse Liver Treated with *Pemt* shRNA and lacZ Control Virus.

Samples	Ob/pemt shRNAi				ob/lacZ RNAi						
Lipid Class (nmol%)	1	2	3	4	1	2	3	4	pemt.ave	lacZ.ave	TTEST
Cholesterol Ester	6.39	1.95	5.11	2.55	1.43	2.22	1.43	3.98	4.00	2.27	0.2017
Diacylglycerol	1.17	1.45	1.51	1.45	1.79	2.60	1.46	1.53	1.40	1.85	0.1515
Free cholesterol	6.96	7.83	7.76	6.84	11.42	7.99	6.86	4.01	7.35	7.57	0.8909
Free fatty acid	2.67	2.59	3.91	3.47	3.37	2.66	2.36	2.26	3.16	2.66	0.2641
Triacylglycerol	11.69	8.57	9.33	13.46	12.33	11.45	19.90	19.76	10.76	15.86	0.0933
Phospholipids	71.13	77.61	72.36	72.22	69.67	73.07	67.98	68.46	73.33	69.79	0.1047
Cardiolipin	9.99	10.12	7.67	8.47	9.26	6.85	7.54	7.73	9.06	7.84	0.1712
Lysophosphatidylcholine	1.77	1.37	1.09	1.25	1.28	1.23	1.15	1.28	1.37	1.23	0.3917
Phosphatidylcholine	30.07	34.20	32.59	35.16	37.46	41.03	37.96	40.60	33.00	39.26	**0.0047**
Phosphatidylethanolamine	24.11	25.46	24.55	21.71	18.09	17.73	17.27	15.65	23.95	17.18	**0.0004**
Phosphatidylserine	5.19	6.46	6.48	5.64	3.59	6.22	4.07	3.21	5.94	4.27	0.0660
PC/PE	1.25	1.34	1.33	1.62	2.07	2.31	2.20	2.60	1.38	2.29	**0.0006**
PC/PS	5.79	5.29	5.04	6.23	10.45	6.60	9.34	12.65	5.59	9.76	**0.0176**

Supplementary Table 5. The Difference in the Fatty Acid Composition of ER Lipids from the Liver of Control and *Pemt* Knockdown ob/ob Mouse.

	Fatty Acids (mol%)	14:0	15:0	16:0	18:0	20:0	22:0	14:1n5	16:1n7	18:1n7	18:1n9	20:1n9	20:3n9	18:2n6	18:3n6	20:2n6	20:3n6	20:4n6	22:4n6	20:5n3	22:5n3	22:6n3	%SFA	%MUFA	%PUFA	%n3	%n6	%n7	%n9
	Cardiolipin	-0.376	NS	NS	2.764	NS	NS	NS	NS	NS	NS	NS	NS	-1.551	NS	NS	NS	-0.149	NS	NS	NS	4.483	NS	NS	3.353	NS	-1.804	NS	NS
	Cholesterol Ester	-6.206	NS	NS	NS	NS	NS	NS	NS	NS	NS	NS	NS	NS	NS	NS	NS	NS	NS	NS	NS	NS	NS	NS	NS	NS	NS	NS	NS
	Diacylglycerol	0.512	NS	4.832	5.737	NS	NS	NS	-1.519	NS	-5.218	NS	NS	NS	NS	NS	NS	NS	NS	NS	NS	-2.148	11.77	-7.932	NS	NS	NS	-2.582	-5.362
	Free fatty acid	1.006	NS	NS	NS	NS	NS	0.183	NS	-0.621	NS	NS	NS	NS	NS	NS	NS	NS	NS	NS	NS	NS	NS	NS	NS	NS	NS	-1.004	NS
ɔid Class	Lysophosphatidylcholine	0.442	NS	NS	NS	NS	NS	NS	NS	NS	NS	NS	-0.197	NS	NS	NS	NS	NS	NS	NS	NS	NS	NS	NS	NS	NS	NS	NS	NS
	Phosphatidylcholine	0.09	0.042	5.739	-3.965	NS	NS	NS	0.427	NS	NS	-0.084	0.089	2.524	NS	-0.086	NS	NS	NS	NS	NS	-5.962	1.979	NS	-4.874	-6.089	NS	NS	NS
	Phosphatidylethanolamine	-0.131	NS	2.482	-2.726	NS	-0.068	NS	NS	NS	NS	NS	NS	1.615	NS	NS	NS	-6.453	NS	NS	0.482	4.345	NS	NS	NS	5.219	-4.579	NS	NS
	Phosphatidylserine	0.281	NS	NS	-4.075	0.127	NS	NS	NS	NS	NS	NS	NS	0.566	NS	NS	NS	-4.518	NS	NS	NS	2.279	NS	NS	NS	NS	-4.121	-0.469	NS
	Triacylglycerol	0.3	NS	NS	NS	NS	NS	NS	NS	-0.943	NS	-0.245	NS	NS	0.076	NS	0.16	0.689	-0.053	0.485	NS	0.836	3.971	-6.2	NS	NS	NS	NS	-5.582

*NS: no significant changes (p>0.05, student t-test); Values are precent mol (mol%) difference between *Pemt* knockdown ob/ob animals and LacZ controls (*Pemt* shRNA - *LacZ* shRNA).

Supplementary Table 6. Oligos Used in This Study

Genes	Orientation	Sequence	Usage
18S	forward	AGCCCCTGCCCTTTGTACACA	q-PCR
18S	reverse	CGATCCGAGGGCCTCACTA	q-PCR
28S	forward	TGTTGACGCGATGTGATTTCTGCC	q-PCR
28S	reverse	AGATGACGAGGCATTTGGCTACCT	q-PCR
Ces3	forward	ATGCGCCTCTACCCTCTGATA	q-PCR
Ces3	reverse	AGCAAATCTCAAGGAGCCAAG	q-PCR
Dak	forward	TCGGGAAAGGGATGCTAACAG	q-PCR
Dak	reverse	CAAGTCCAAAGTTGAGCCGAT	q-PCR
Dgat2	forward	GCGCTACTTCCGAGACTACTT	q-PCR
Dgat2	reverse	GGGCCTTATGCCAGGAAACT	q-PCR
Fas	forward	TATCAAGGAGGCCCATTTTGC	q-PCR
Fas	reverse	TGTTTCCACTTCTAAACCATGCT	q-PCR
Herpud1	forward	CTGGGGACTCCTCAAGTGATG	q-PCR
Herpud1	reverse	ACGTTGTGTAGCCAGAGAAGC	q-PCR
LacZ	top	CACCGCTACACAAATCAGCGATTTCGAAAAATCGCTGATTTGTGTAG	shRNA
LacZ	bottom	AAAACTACACAAATCAGCGATTTTTCGAAATCGCTGATTTGTGTAGC	shRNA
Mttp	forward	ATACAAGCTCACGTACTCCACT	q-PCR
Mttp	reverse	TCCACAGTAACACAACGTCCA	q-PCR
Pcyt1a	forward	GATGCACAGAGTTCAGCTAAAGT	q-PCR
Pcyt1a	reverse	TGGCTGCCGTAAACCAACTG	q-PCR
Pcyt2	forward	TGTGTTCACGGCAATGACATC	q-PCR
Pcyt2	reverse	TTCCCGGTACTCAGAGGACAT	q-PCR
Pemt	forward	TTGGGGATTCGTGTTTGTGCT	q-PCR
Pemt	reverse	CACGCTGAAGGGAAATGTGG	q-PCR
Ptdss1	forward	GCAGGACTCTGAGCAAGGATG	q-PCR
Ptdss1	reverse	GGCGAAGTACATGAGGCTGAT	q-PCR
Ptdss2	forward	GGATTGCCTTTCAGTTCACGC	q-PCR
Ptdss2	reverse	AGGTAGAAGGTGTTCAGCTCTG	q-PCR
Scd1	forward	TTCTTGCGATACACTCTGGTGC	q-PCR
Scd1	reverse	CGGGATTGAATGTTCTTGTCGT	q-PCR
Serca2 (Atp2a2)	forward	CATGCACCGATGGGATTTCCT	q-PCR
Serca2 (Atp2a2)	reverse	CGCTAAAGTTAGTGTCTGTGCT	q-PCR
Pemt	top	CACCGCCATGTCCCGACACACTAACTCGAGTTAGTGTGTCGGGACATGG	shRNA
Pemt	bottom	AAAACCATGTCCCGACACACTAACTCGAGTTAGTGTGTCGGGACATGGC	shRNA
Serca2b	forward	CACCGCCGTTTGTAATTCTGCTTATCTCGAGATAAGCAGAATTACAAACGGC	shRNA
Serca2b	reverse	AAAAAGCCGTTTGTAATTCTGCTTATCTCGAGATAAGCAGAATTACAAACGGC	shRNA
Serca2b	forward	GCCATGGAGAACGCGCACAC	ORF cloning
Serca2b	reverse	AGACCAGAACATATCGCTAAAGTTAG	ORF cloning